EXPERIMENTAL AND MODELING STUDY OF DIAUXIC LAG IN BACTERIA SWITCHING BETWEEN ELECTRON ACCEPTORS

By

PI-HSIN LIU

A DISSERTATION PRESENTED TO THE GRADUATE SCHOOL
OF THE UNIVERSITY OF FLORIDA IN PARTIAL FULFILLMENT
OF THE REQUIREMENTS FOR THE DEGREE OF
DOCTOR OF PHILOSOPHY

UNIVERSITY OF FLORIDA

1998

This dissertation

is dedicated

to my parents

ACKNOWLEDGMENTS

There are many who have helped me throughout my education in the University of Florida, but none more so than my committee chairmen, Professors Spyros A. Svoronos and Ben Koopman. They are always available and willing to discuss ideas. Their guidance during the research was invaluable and I appreciate all of their help. I would also like to thank the other members of my committee, Professors Richard Dickinson, Dale Kirmse, Gar Hoflund, and Paul A. Chadik for their interest and suggestions in this project and my academic career. In addition to my committee members, Professor Oscar Crisalle is thanked for his guidance.

I would like to thank several graduate students in the Department of Chemical Engineering and Department of Environmental Engineering Sciences: Wilbur Woo, Maria Luisa Jones, Sanjay Gupta, and Guogen Zhan. They have helped me in a variety of ways during my work with their knowledge and friendship.

Finally, I would like to thank my parents, sisters (especially my younger sister Pi-Hsuan Liu), and my best friend Da-Wei Lin for their love and continual support during my years in University of Florida.

TABLE OF CONTENTS

page

ACKNOWLEDGMENTS iiii

ABSTRACT v

CHAPTERS

1 INTRODUCTION 1

2 DIAUXIE OF ACTIVATED SLUDGE 3
  2.1 Introduction 3
  2.2 Experimental Methods 5
    2.2.1 Activated Sludge and Enrichment Cultures 5
    2.2.2 Growth Experiments 6
    2.2.3 Analytical Methods 6
  2.3 Experimental Results 8
  2.4 Modeling 22
  2.5 Discussion 34

3 DIAUXIE OF *PSUDOMONAS DENITRIFICANS* 37
  3.1 Introduction 37
  3.2 Experimental Methods 39
    3.2.1 Growth Experiments 40
    3.2.2 Experimental Protocol 40
    3.2.3 Analytical Methods 42
  3.3 Experimental Results 43
  3.4 Modeling 50
  3.5 Conclusions 63

4 CONCLUSIONS AND FUTURE WORK 66

LIST OF REFERENCES 68

BIOGRAPHICAL SKETCH 71

Abstract of Dissertation Presented to the Graduate School
of the University of Florida in Partial Fulfillment of the
Requirements for the Degree of Doctor of Philosophy

EXPERIMENTAL AND MODELING STUDY OF DIAUXIC LAG IN BACTERIA SWITCHING BETWEEN ELECTRON ACCEPTORS

By

PI-HSIN LIU

May, 1998

Chairman: Spyros Svoronos
CoChairman: Ben Koopman
Major Department: Chemical Engineering

We have shown experimentally that a diauxic lag can be exhibited when activated sludge bacteria switch from oxygen to nitrate as electron acceptors. This behavior was successfully modeled using a cybernetic modification of the "industry standard" IAWQ Activated Sludge Model 1. The new model correctly predicts oxygen and nitrate uptake as well as the growth pattern and diauxie. It shows that diauxie occurs when the specific level of denitrifying enzyme is low at the outset of the anoxic phase, whereas if the specific level is initially high, a diauxie will not be observed. The present work suggests that caution is needed in the application of conventional models for optimizing periodic processes for nitrogen removal, especially when the phase lengths considered are either much shorter or much longer than those tested under experimental conditions.

We have also shown that *Pseudomonas denitrificans* undergo a diauxie when switching from dissolved oxygen to nitrate as terminal electron acceptor. The length of time under aeration significantly affected the length of diauxic lag, whereas the presence or absence of nitrate in the culture under aeration had a marginal effect. Nitrate consumption was very low during the lag period, then increased rapidly, coinciding with exponentially increasing biomass. The previously developed model could not satisfactorily portray the dependence of diauxic lag length on the duration of the preceding aerated phase. It was therefore modified with new expressions for enzyme synthesis and enzyme activity. The revised model successfully predicts the different lengths of diauxic lags observed in the experiments as well as the growth pattern and nitrate uptake.

CHAPTER 1
INTRODUCTION

The phenomenon of diauxie is first discovered by Monod in 1942. It happens when bacteria have choices of two carbon sources, e.g. glucose and sorbitol, bacteria will consume glucose first which supports the faster growth. Until glucose is exhausted, bacteria then begin to utilize sorbitol. This usually results a lag which defines as diauxic lag of little or no growth between the time that the first carbon source (glucose) is exhausted and exponential growth begins on the second carbon source (sorbitol).

Diauxie is also discovered by Kodama in 1969 when *Pseudomonas stutzeri* switches between nitrate to nitrite as terminal electron acceptor. In this study, we observed that diauxie happens when bacteria switch from oxygen to nitrate as electron acceptor. This is observed in tests with activated sludge from a full-scale biological process for nitrogen removal (the Bio-Denipho®[†] process at the University of Florida), enrichment cultures (inoculated from activated sludge), and with pure culture (*Pseudomonas denitrificans*). This may have significant engineering and economic implications since several wastewater treatment processes for nitrogen removal (e.g., sequencing batch reactors, the Bio-Denitro process, and the Bio-Denipho process) periodically switch between oxygen and nitrate as the terminal electron acceptor. We also carry out experiments with *P. denitrificans* to investigate the factors which affect the length of diauxic lag. The length of the aeration period is resulted to have significant effect on the length of diauxic lag, whereas the presence or absence of nitrate during aerating phase has marginal effect on the length of diauxic lag.

[†] The Bio-Denipho® process is a patented process developed by I Krüger Systems in cooperation with the Department of Environmental Engineering at the Technical University of Denmark (Isaacs *et al.*, 1994).

Diauxic lag caused by changing between carbon sources has been successfully modeled using a cybernetic model (Kompala *et al.*, 1986). "Industry standard" IAWQ Activated Sludge Models No. 1 and 2 (Henze *et al.*, 1987; 1995) do not account for any diauxic lag when bacteria switch between oxygen to nitrate as electron acceptor. In order to portray the observed diauxies, we first developed a cybernetic approach which incorporates with the industry-standard activated sludge model No. 1. This cybernetic approach is able to predict the diauxic lags observed with activated sludge, however, cannot satisfactorily fit the considerably longer lags observed with pure culture. A new model accounting for enzyme synthesis and activity in response to culture conditions and enzyme specific levels is then developed. It successfully predicts the very long diauxic lag observed in the pure culture experiments as well as the different lengths of diauxic lags, the growth pattern, and nitrate uptake.

CHAPTER 2
DIAUXIE OF ACTIVATED SLUDGE

2.1 Introduction

With increasing demands placed on wastewater treatment plants to achieve higher degrees of purification in a cost-effective manner and a growing emphasis on nitrogen removal, cyclic processes are becoming increasingly popular. This stems from their adaptability to a wide range of operating conditions, wastewater compositions, and influent flow rates. Nitrogen removal is achieved in cyclic processes by operating treatment reactors alternately in aerated (nitrifying) and unaerated (denitrifying) phases. Such operation forces the biomass to switch between electron acceptors, i.e., between dissolved oxygen under aerated conditions and nitrate under unaerated conditions. The relative lengths of the phases can be varied to compensate for varying conditions. Also, the frequency of cycling has proven to be useful as an adjustable variable in optimizing the operation of cyclic processes (Potter *et al.*, 1996).

It is known that bacteria switching between electron donors (carbon substrates) go through a lag phase caused by adjustment of intracellular enzyme levels (Monod, 1942; 1949). Under conditions allowing exponential growth, the bacteria prefer to consume the substrate that supports the faster growth rate, resulting in the sequential utilization of substrates. Only when the faster growth-supporting substrate is exhausted do they begin to utilize the second substrate. This usually results in a lag period (the *diauxie*) of little or no growth between the time that the first substrate is exhausted and exponential growth begins on the second substrate.

The question may be posed as to whether or not bacteria switching between electron *acceptors* go through a similar diauxic lag. This has significant engineering and economic implications for cyclic biological nitrogen processes. If a lag period results from such switchovers (e.g., oxygen to nitrate as electron acceptors), then increasing the number of such switches (i.e., the frequency of cycling) between aerated and unaerated conditions would have an adverse impact on the overall rate of nitrogen removal achieved by the facility. Well-accepted models of single-sludge processes such as the IAWQ Activated Sludge Model Nos. 1 and 2 (Henze *et al.*, 1987; 1995) do not account for any lag when bacteria switch between electron acceptors.

In the present work it is shown that with glucose present in nonlimiting concentrations, activated sludge exhibits a diauxic lag when switching from oxygen to nitrate as the terminal electron acceptor. This was observed both in tests with activated sludge from a full-scale biological process for nitrogen removal (the Bio-Denipho® process at the University of Florida) and in tests with enrichment cultures inoculated with activated sludge from the same process. Using the cybernetic approach of Kompala *et al.* (1986), we modified the Activated Sludge Model No. 1 so that it could successfully depict the diauxic lag observed when activated sludge switches from oxygen to nitrate as electron acceptor.

2.2 Experimental Methods

2.2.1 Activated Sludge and Enrichment Cultures

Activated sludge or seed bacteria for enrichment cultures were obtained from the Bio-Denipho process at the University of Florida (UF). This process consists of two parallel trains (east and west), each with an anaerobic reactor, parallel oxidation ditches which alternated between anoxic and oxic conditions, a final anoxic reactor, and a final aerated reactor. The sampling point was at the entry to the final anoxic reactor of the west train.

In experiments using plant biomass without enrichment, a sample of activated sludge from the final anoxic reactor was blended for 20 seconds, settled for 10 min to remove large particles, and 4.0 L of supernatant was collected. The supernatant was transferred to a glass culture bottle and used immediately.

Enrichment cultures were developed by settling a sample of mixed liquor for 1 hour, collecting 4 L supernatant, and adding nutrients and buffer [1250 mg/L glucose, 10 mg/L nitrate N (KNO_3), 5 mg/L phosphate P (KH_2PO_4), 10 mg/L ammonia N (NH_4CL), 100 mg/L sodium bicarbonate]. Nitrification inhibitor (N-Hib, Hach Co.) was added at a dosage of 500 mg/L. The culture was subjected to oxic/anoxic cycling (60 min/60 min) over a period of 1 to 7 days in a glass bottle having a liquid volume of 4.0 L. Each day, 1.0 L of mixed culture volume was replaced with 1.0 L of settled supernatant from Bio-Denipho mixed liquor generated as described above. The added supernatant was dosed with nutrients at the concentrations given above. Trace nutrients were assumed to be provided by the activated sludge supernatant from the plant. Enrichment cultures were incubated at approximately 28 °C. The pH of the medium was 7.2-7.5.

2.2.2 Growth Experiments

A total of thirteen growth experiments were carried out, five with plant biomass and eight with enrichment cultures (Table 2.1). Each experiment consisted of a preliminary aeration period of varying length (usually 2 hours) in which the dissolved oxygen (DO) concentration reached 8 mg/L or higher, followed by a period of mixing without aeration. The time at which aeration was stopped is referred to as time zero in Table 2.1. Nutrients were added at various times and in various dosages. After aeration was stopped, the head space of the culture bottle was flooded continuously with nitrogen gas to minimize oxygen intrusion. Measurements of chemical oxygen demand (COD) were carried out as needed to ensure that the carbon source (glucose) was present in excess at the beginning of the unaerated period in every experiment. Other variables monitored included biomass in terms of absorbance and dry weight, dissolved oxygen, nitrate, and nitrite. All experiments were carried out at approximately 28 °C.

2.2.3 Analytical Methods

Samples were withdrawn from the reactor using a syringe connected to a plastic tube that extended through the cap to the bottom of the reactor. The sample line was initially flushed several times, then 30 mL of culture was withdrawn. A portion (20 mL) of each sample was immediately passed through a membrane filter (Gelman GN-6) having

Table 2.1. Experimental conditions

Exp. Number	Length of preliminary aeration period, hr	Times of nutrient additions[†]	Dosed Concentrations (mg/L)						
			Glucose	NO_3 -N	NH_4 -N	PO_4-P	Fe^{2+}	$NaHCO_3$ buffer solution	Nitrification Inhibitor
P-1[#]	2.0	0	500	10	100	5	1.25	75	500
P-2	2.0	0	500	10	100	5	1.25	75	500
P-3	5.5	- 5.5	500	10	100	5	1.25	75	500
P-4	6.0	- 6.0	500	10	100	5	1.25	75	500
P-5	7.0	- 7.0	500	10	100	5	1.25	75	500
		0	120				0.25	20	100
E-1[*]	2.0	0	300	20	20	10	1.25	62.5	500
E-2	2.0	0	2050	10	10	5	1.25	100	500
E-3	2.0	0	2000	10	10	5	1.25	75	500
E-4	2.0	0	2000	10	10	5	1.25	75	500
E-5	2.0	0	500	900	100	25	1.25	75	500
E-6	2.0	0	2000	10	10	5	1.25	75	500
E-7	2.0	-2	500						
		0	322.5	10	10	5	1.25	75	500
E-8	2.0	-2	500						
		0	322.5	10	10	5	1.25	75	500

[†] Time 0 is the time at which aeration was turned off.

[#] Biomass was taken from the UF Bio-Denipho process.

[*] Biomass was taken from an enrichment culture.

an effective pore size of 0.45 μm and the filtrates were stored at 4°C. The remainder (unfiltered portion) of the sample was used for absorbance and dry weight measurements.

Absorbance of the culture was measured with a spectrophotometer (Milton Roy Spectronic 21D) at 750 nm using a 1.25 cm path length. Dry weight concentrations of culture were measured on membrane filters (0.45 μm effective pore size) after drying to constant weight at 103 °C.

COD, nitrate and nitrite were measured using test kits (Hach): low range (0 - 150 mg/L) COD test vials, Test 'N Tube NitraVerX nitrate reagent sets (0 - 30 mg/L), and Test 'N Tube NitriVer3 nitrite test vials (0 - 0.5 mg/L). Absorbance was measured at 420 nm for COD, at 410 nm for nitrate and at 507 nm for nitrite. Calibration curves were made up for each new set of reagents. Dissolved oxygen was measured using a YSI model 57 DO meter.

2.3 Experimental Results

Results of the experiments with plant biomass are shown in Figure 2.1 - Figure 2.5 and with the enrichment cultures in Figure 2.6 - Figure 2.13. The solid lines show biomass concentration as indicated by absorbance and the dashed lines show dissolved oxygen concentration. In all the experiments the nitrate nitrogen concentration exceeded 8 mg/L at the time that DO ran out and the diauxie began. This value is much greater than the typical half-saturation coefficient for anoxic growth on nitrate. For example, in test P-1 (Figure 2.1) we observed that during the first 4.5 hrs absorbance increases with an accompanying drop of DO toward zero. For the next 1.8 hrs absorbance stays flat, i.e.,

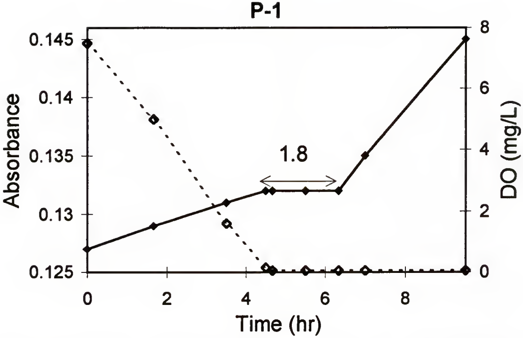

Figure 2.1: Temporal variation of absorbance (solid lines) and dissolved oxygen concentration (dashed lines) in batch experiment started with activated sludge from the University of Florida Bio-Denipho facility. The double-headed arrows indicate the lengths of diauxic lag periods.

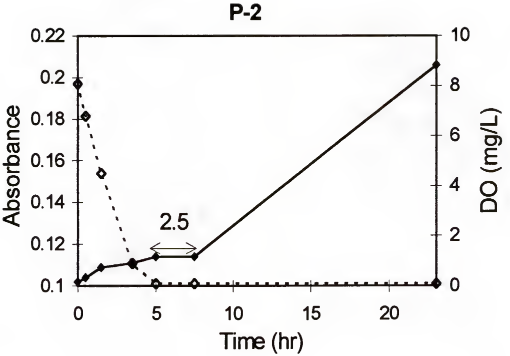

Figure 2.2: Temporal variation of absorbance (solid lines) and dissolved oxygen concentration (dashed lines) in batch experiment started with activated sludge from the University of Florida Bio-Denipho facility. The double-headed arrows indicate the lengths of diauxic lag periods.

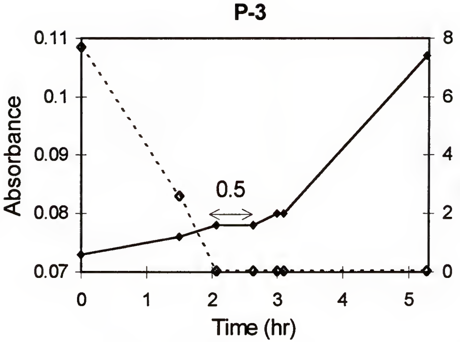

Figure 2.3: Temporal variation of absorbance (solid lines) and dissolved oxygen concentration (dashed lines) in batch experiment started with activated sludge from the University of Florida Bio-Denipho facility. The double-headed arrows indicate the lengths of diauxic lag periods.

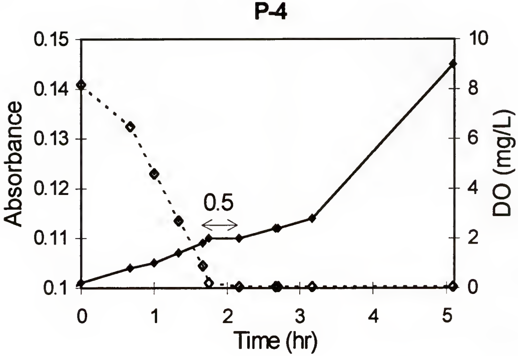

Figure 2.4: Temporal variation of absorbance (solid lines) and dissolved oxygen concentration (dashed lines) in batch experiment started with activated sludge from the University of Florida Bio-Denipho facility. The double-headed arrows indicate the lengths of diauxic lag periods.

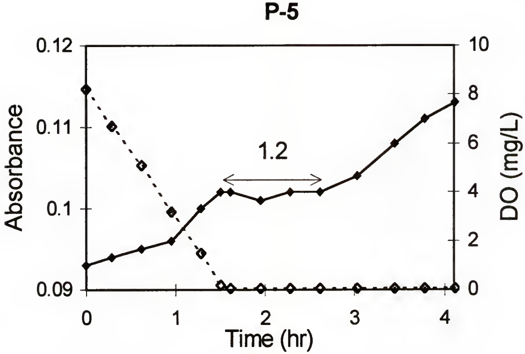

Figure 2.5: Temporal variation of absorbance (solid lines) and dissolved oxygen concentration (dashed lines) in batch experiment started with activated sludge from the University of Florida Bio-Denipho facility. The double-headed arrows indicate the lengths of diauxic lag periods.

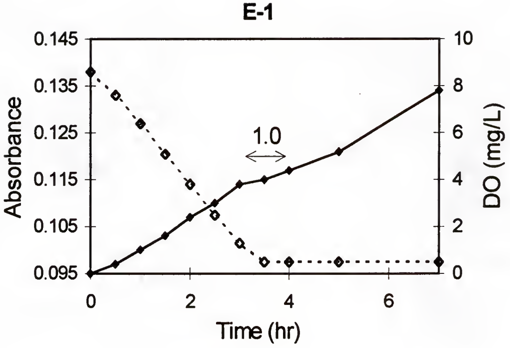

Figure 2.6: Temporal variation of absorbance (solid lines) and dissolved oxygen concentration (dashed lines) in batch experiment started with enrichment culture. The double-headed arrows indicate the lengths of diauxic lag periods.

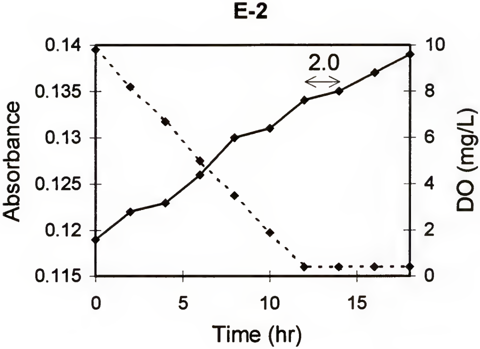

Figure 2.7: Temporal variation of absorbance (solid lines) and dissolved oxygen concentration (dashed lines) in batch experiment started with enrichment culture. The double-headed arrows indicate the lengths of diauxic lag periods.

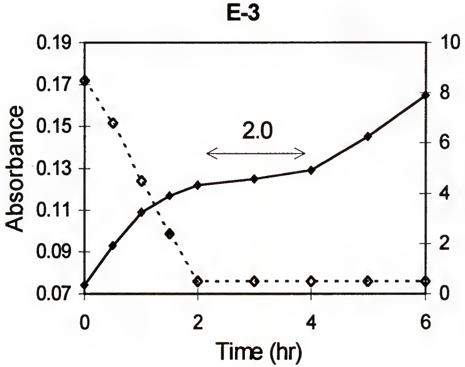

Figure 2.8: Temporal variation of absorbance (solid lines) and dissolved oxygen concentration (dashed lines) in batch experiment started with enrichment culture. The double-headed arrows indicate the lengths of diauxic lag periods.

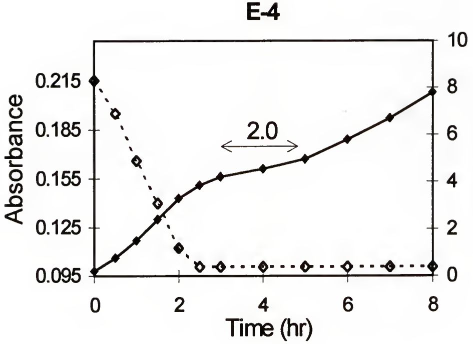

Figure 2.9: Temporal variation of absorbance (solid lines) and dissolved oxygen concentration (dashed lines) in batch experiment started with enrichment culture. The double-headed arrows indicate the lengths of diauxic lag periods.

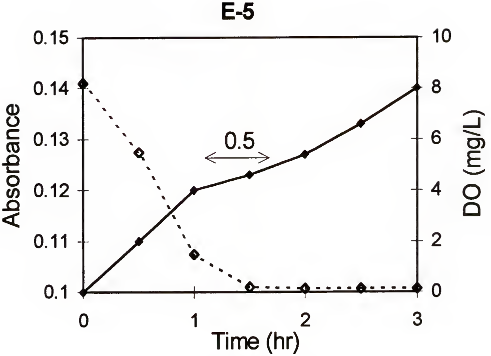

Figure 2.10: Temporal variation of absorbance (solid lines) and dissolved oxygen concentration (dashed lines) in batch experiment started with enrichment culture. The double-headed arrows indicate the lengths of diauxic lag periods.

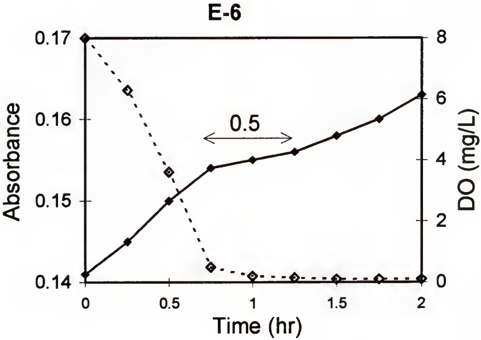

Figure 2.11: Temporal variation of absorbance (solid lines) and dissolved oxygen concentration (dashed lines) in batch experiment started with enrichment culture. The double-headed arrows indicate the lengths of diauxic lag periods.

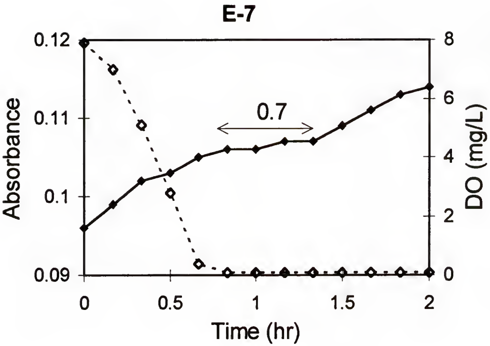

Figure 2.12: Temporal variation of absorbance (solid lines) and dissolved oxygen concentration (dashed lines) in batch experiment started with enrichment culture. The double-headed arrows indicate the lengths of diauxic lag periods.

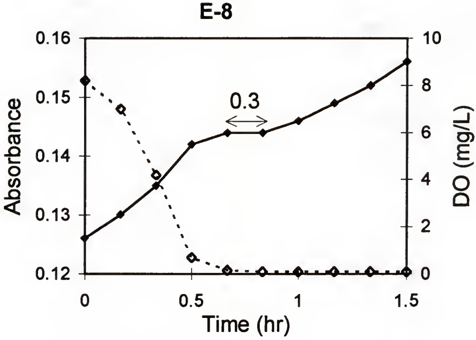

Figure 2.13: Temporal variation of absorbance (solid lines) and dissolved oxygen concentration (dashed lines) in batch experiment started with enrichment culture. The double-headed arrows indicate the lengths of diauxic lag periods.

there is no appreciable growth. This period of reduced growth rate (zero in this case) is the diauxic lag. Subsequently, exponential growth resumes. Similar behavior was also observed in the other four tests (Figure 2.2 - Figure 2.5) with plant biomass; in each case, as DO approached zero, growth rate fell to close to zero for a period of time. Five of the eight tests with enrichment cultures (Figure 2.8, Figure 2.9, and Figure 2.11 - Figure 2.13) showed periods of very low (nearly zero) growth rate which can be clearly identified as diauxies. In the other three runs (Figure 2.6, Figure 2.7, and Figure 2.10), when DO approached zero the growth rate dropped somewhat but did not approach zero. As such a change in growth rate can also be explained by a lower maximum specific growth rate on nitrate, the existence of a diauxic lag is not deemed conclusive in these three runs.

Estimates of the lengths of the diauxic lag periods in Figures 2.1 - Figure 2.13 are indicated by the double-arrowed lines. These estimates ranged from 0.3 to 2.5 hours. The average of the five runs with unenriched plant biomass (1.3 hrs) was close to the average of the five conclusive diauxies with enrichment culture (1.1 hrs). This length of time is quite significant when compared to the typical cycle length of 2 hrs in a periodic process, e.g. the Bio-Denipho process (Zhao *et al.*, 1994).

2.4 Modeling

In the "industry standard" models for activated sludge (ASM-1, Henze et al., 1987; ASM-2, Henze et al., 1995), the effect of dissolved oxygen on the rate of growth of heterotrophic biomass under anoxic conditions is represented by the term,

$$\frac{K_{O,H}}{S_O + K_{O,H}} \qquad (1)$$

whereas the rate of heterotrophic growth under aerobic conditions is controlled by the term

$$\frac{S_O}{S_O + K_{O,H}} \tag{2}$$

where S_O is the dissolved oxygen concentration and $K_{O,H}$ the oxygen half-saturation coefficient. The former term approaches zero when dissolved oxygen concentration is high, and approaches 1.0 when dissolved oxygen concentration is low. The latter term has complementary behavior, approaching 1.0 when DO is high and tending towards zero when DO is low. Together, the two terms sum always to 1.0, thus ensuring that the total rate of growth using both electron acceptors does not exceed that which is possible in a highly aerobic environment. This feature, however, prevents either model from accurately portraying the dramatic decrease or even cessation of growth during the diauxie.

An example of a conventional model of heterotrophic growth under aerobic and anoxic conditions is shown in Table 2.2.

Table 2.2. Conventional model of heterotrophic growth under aerobic and anoxic conditions

Component→	i	1	2	3	
j	Process ↓	S_o	S_{NO}	$X_{B,H}$	Process rate, ρ_j, $ML^{-3}T^{-1}$
1	Aerobic growth of heterotrophs	$-\frac{1-Y_{H,O}}{Y_{H,O}}$		1	$\hat{\mu}_{H,O}\left(\frac{S_O}{K_{O,H}+S_O}\right)X_{B,H}$
2	Anoxic growth of heterotrophs		$-\frac{1-Y_{H,NO}}{2.86Y_{H,NO}}$	1	$\hat{\mu}_{H,NO}\left(\frac{K_{O,H}}{K_{O,H}+S_O}\right)\left(\frac{S_{NO}}{K_{NO}+S_{NO}}\right)X_{B,H}$
3	Decay of heterotrophs			-1	$b_H X_{B,H}$
Observed conversion rate, $ML^{-3}T^{-1}$		$r_i = \sum_j \gamma_{ij}\rho_j$			

The model, which is a simplified version of ASM-1, contains process rate expressions for aerobic growth of heterotrophic biomass, anoxic growth of heterotrophic biomass, and decay of heterotrophic biomass. The components include active heterotrophic biomass ($X_{B,H}$), dissolved oxygen (S_O), and the sum of nitrate plus nitrite nitrogen expressed as equivalent nitrate (S_{NO}) by the following equation:

$$S_{NO} = [NO_3 - N] + \frac{(2.857 - 1.143)}{2.857}[NO_2 - N] \tag{3}$$

Note that neither of the process rate expressions for growth contains a substrate concentration term, nor is substrate shown as a component. This is because the carbon source (glucose) was present in excess in experiment P-5 (Figure 2.5), as it was in all experiments.

To demonstrate typical behavior of conventional models, we fitted the model from Table 2.2 to the data from one of the experiments that used plant biomass (P-5, Figure 2.5). A diauxic lag of 1.2 hours was measured in this experiment, which is close to the average. In the fitting, values for the parameters $K_{O,H}$ (half-saturation coefficient for oxygen) and K_{NO} (half-saturation coefficient for nitrate) were taken from earlier infinite dilution experiments carried out according to the procedure of Williamson and McCarty (1975). The remaining model parameters (maximum specific growth rate with oxygen $\hat{\mu}_{H,O}$, maximum specific growth with nitrate $\hat{\mu}_{H,NO}$, yield coefficients $Y_{H,O}$ and $Y_{H,NO}$, and decay rate b_H) as well as the initial concentration of active heterotrophic biomass and inert particulate matter were determined by nonlinear weighted least squares fitting using the following performance measure:

$$J = \frac{1}{\sigma_{S_O}^2}\sum_i (S_{Omeas,i} - S_{Opred,i})^2 + \frac{1}{\sigma_{S_{NO}}^2}\sum_j (S_{NOmeas,j} - S_{NOpred,j})^2 + \frac{1}{\sigma_A^2}\sum_\ell (A_{meas,\ell} - A_{pred,\ell})^2 \quad (4)$$

where $\sigma_{S_O} = 0.1\ mg/L$, $\sigma_{S_{NO}} = 0.5\,mg/L$, and $\sigma_A = 0.02$ are the standard deviations of the dissolved oxygen, nitrate-nitrogen and absorbance (A) measurements, respectively. The parameter values are shown in Table 2.3.

Results of the fitting are shown in Figure 2.14 and Figure 2.15. In Figure 2.14, the same yield coefficient is used for growth on either dissolved oxygen or nitrate, as assumed by default ASM-1. The model in this case does not match the growth rates under DO and nitrate, giving a higher than observed growth rate for DO and a lower than observed growth rate for nitrate. If the yields under aerobic and anoxic conditions are allowed to differ, the conventional model is able to match both growth rates. Nevertheless, it still fails to depict the diauxic lag (Figure 2.15). Parameter values for both fits are given in Table 2.3. Clearly, a new modeling approach is needed to successfully portray the diauxie.

Cybernetic modeling (Ramkrishna, 1982; Ramkrishna *et al.*, 1984; Kompala *et al.*, 1986; Straight and Ramkrishna, 1991; Straight and Ramkrishna, 1994; Ramakrishna *et al.*, 1995) has been successful in portraying the diauxic lag observed when bacteria switch between electron donors. It is based on the premise that bacteria are optimal strategists (Ramkrishna *et al.*, 1987) and that they therefore regulate enzyme synthesis and activity so as to maximize their specific growth rate. In the following, we modify the kinetic

Table 2.3. Parameter values in the models

Parameter	Symbol	Units	Conventional model		Cybernetic model
			Same yield	Diff. yield	
Maximum Specific Rates					
Growth in DO	$\hat{\mu}_{H,O}$	hr^{-1}	0.669	0.646	0.787
Growth in nitrate	$\hat{\mu}_{H,NO}$	hr^{-1}	0.220	0.489	0.639
Yields					
in DO phase	$Y_{H,O}$	g cell COD / g substrate COD	0.677	0.515	0.612
in nitrate phase	$Y_{H,NO}$	g cell COD / g substrate COD	0.677	0.805	0.809
Half Saturation Coefficients					
Oxygen coeff.	$K_{O,H}$	g O_2 m^{-3}	0.277	0.277	0.277
Nitrate coeff.	K_{NO}	g NO_3-N m^{-3}	1.0	1.0	1.0
Biomass Specific Decay Rate	b_H	hr^{-1}	0.0042	0.0024	0.0024
Initial Active Biomass Concentration	$X_{Active}(-7)$*	g COD m^{-3}	0.174	0.0997	0.0514
Initial Inert Biomass Concentration	$X_{Inert}(-7)$	g COD m^{-3}	179.32	181.33	181.34
Initial Specific Enzyme Levels					
DO	$e_O(-7)$	g enzyme / g biomass			0.00118
Nitrate	$e_{NO}(-7)$	g enzyme / g biomass			0.00014
Enzyme Specific Synthesis Rates					
DO	α_O	hr^{-1}			0.00099
Nitrate	α_{NO}	hr^{-1}			0.00175
Enzyme Specific Decay Rates					
DO	β_O	hr^{-1}			0.05
Nitrate	β_{NO}	hr^{-1}			0.05

*Level at time equal to -7 hr.

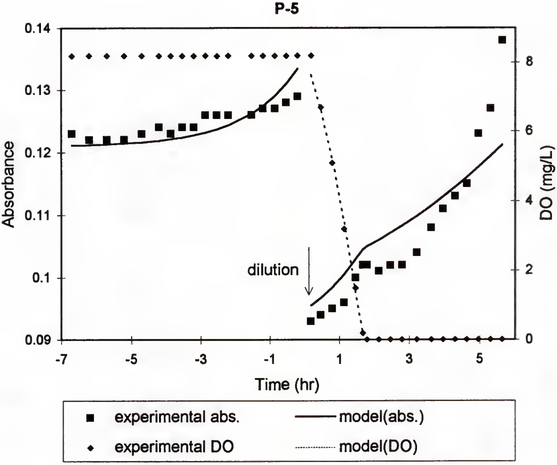

Figure 2.14: Conventional model fits to P-5 experimental data using the same value of Y_H in the DO and nitrate growth phases. The discontinuity seen at time zero is due to dilution of the culture.

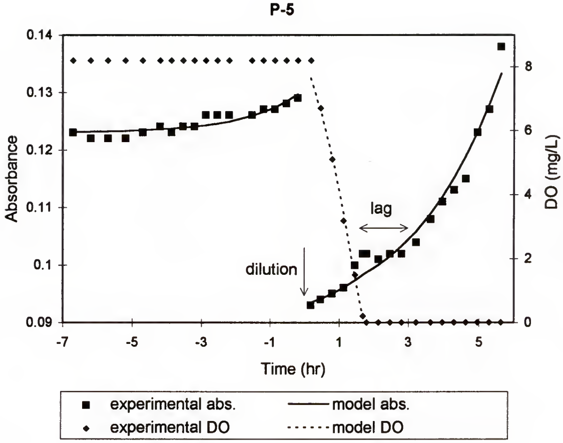

Figure 2.15: Conventional model fits to P-5 experimental data using different values of Y_H for the DO and nitrate phases. The discontinuity seen at time zero is due to dilution of the culture.

expressions of Table 2.2 in a manner analogous to the modifications of Monod kinetic expressions by Kompala *et al.* (1986).

The diauxic lag is attributed to the fact that appropriate enzymes for utilizing alternate electron acceptors must be synthesized. Therefore the new model adds as components the concentrations of two enzymes, E_O and E_{NO}, that regulate biomass synthesis in the presence of oxygen and nitrate, respectively. Both the concentrations and activities of these enzymes affect the growth rate of heterotrophic biomass. If e_k denotes the specific level of an enzyme [i.e., $e_k = E_k/X_{B,H}$ for k = O (oxygen) or NO (equivalent nitrate)] and v_k denotes relative activity (ranging from 0 to 1) of the respective enzymes, then the effects of enzyme level and activity on biomass growth rate can be expressed by multiplying a Monod growth rate expression by the factor $v_k\, e_k/e_{k,max}$, where $e_{k,max}$ is the enzyme maximum specific level. This gives the following equations for aerobic or anoxic growth:

$$\rho_k = \hat{\mu}_{H,k} \frac{e_k\, v_k}{e_{k,max}} \left(\frac{S_k}{K_k + S_k} \right) X_{B,H} \tag{5}$$

where $K_O = K_{O,H}$.

It is postulated that the synthesis rate of each enzyme can be described by the expression

$$\alpha_k\, u_k \left(\frac{S_k}{K_k + S_k} \right) X_{B,H} \tag{6}$$

in which the maximum specific synthesis rate depends on a “cybernetic” variable u_k (ranging from 0 to 1) that controls whether the enzyme is synthesized or not and at what rate, and α_k is a synthesis rate coefficient.

Enzyme decay is assumed to be first order with respect to enzyme concentration, in a manner analogous to biomass decay, i.e. the decay rate is

$$\beta_k E_k \tag{7}$$

In the above formulation the variables u_k and v_k represent the control actions of the cellular regulatory processes of repression-induction and inhibition-activation. In the cybernetic modeling approach it is postulated that the bacteria adjust the values of these variables, as well as of $e_{k,max}$, so as to maximize their instantaneous growth rate. As shown by Kompala *et al.* (1986), the solution of the optimization problem is:

$$u_k = \frac{\rho_k / v_k}{\sum_{k=1}^{2} (\rho_k / v_k)} \tag{8}$$

$$v_k = \frac{\rho_k / v_k}{\max_k (\rho_k / v_k)} \tag{9}$$

$$e_{k,\max} = \frac{\alpha_k}{\hat{\mu}_{H,k} + \beta_k} \tag{10}$$

The complete kinetic model is summarized in Table 2.4. It should be noted that the term $K_{O,H}/(K_{O,H} + S_O)$, which is used in ASM-1 and ASM-2 to switch off growth on nitrate when oxygen is present, is not included, as v_{NO} assumes this function.

As Figure 2.16 and Figure 2.17 shows, the new model fits the absorbance, dissolved oxygen and nitrate data of Experiment P-5 quite well. As before, $K_{O,H}$ and K_{NO} were the experimentally determined values. The enzyme decay coefficients were set equal to the default values used in Kompala *et al.* (1986) and the unknown parameters and initial

Table 2.4. Process kinetics and stoichiometry of the cybernetic model proposed in the present work

Component→	i	1	2	3	4	5	
j	Process ↓	S_O	S_{NO}	$X_{B,H}$	E_O	E_{NO}	Process rate, ρ_j, $ML^{-3}T^{-1}$
1	Aerobic growth of heterotrophs	$-\frac{1-Y_{H,O}}{Y_{H,O}}$		1			$\hat{\mu}_{H,O}\frac{e_O v_O}{e_{O,max}}\left(\frac{S_O}{K_{OH}+S_O}\right)X_{BH}$
2	Anoxic growth of heterotrophs		$-\frac{1-Y_{H,NO}}{2.86Y_{H,NO}}$	1			$\hat{\mu}_{H,NO}\frac{e_{NO} v_{NO}}{e_{NO,max}}\left(\frac{S_{NO}}{K_{NO}+S_{NO}}\right)X_{BH}$
3	Decay of heterotrophs			-1			$b_H X_{B,H}$
4	Synthesis rate of enzyme associated with aerobic growth				1		$\alpha_O\left(\frac{S_O}{K_{OH}+S_O}\right)X_{BH}u_O$
5	Synthesis rate of enzyme associated with anoxic growth					1	$\alpha_{NO}\left(\frac{S_{NO}}{K_{NO}+S_{NO}}\right)X_{BH}u_{NO}$
6	Enzyme decay rate				-1		$\beta_O E_O$
7	Enzyme decay rate					-1	$\beta_{NO} E_{NO}$
Observed conversion rate, $ML^{-3}T^{-1}$		$r_i=\sum_j \gamma_{ij}\rho_j$					

Model Relationships

$$v_i = \frac{\rho_i / v_i}{\max_i(\rho_i / v_i)}$$

$$u_i = \frac{\rho_i / v_i}{\sum_{i=1}^{2}(\rho_i / v_i)}$$

$$e_i = \frac{E_i}{X_{B,H}}$$

$$e_{i,max} = \frac{\alpha_i}{\mu_{max,i}+\beta_i}$$

where

$i = O$ or NO

$\rho_O = \rho_1$

$\rho_{NO} = \rho_2$

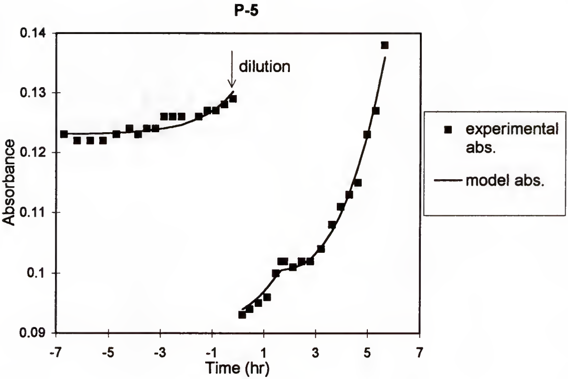

Figure 2.16: Cybernetic model fit to P-5 experimental data: absorbance. The discontinuity seen at time zero is due to dilution of the culture.

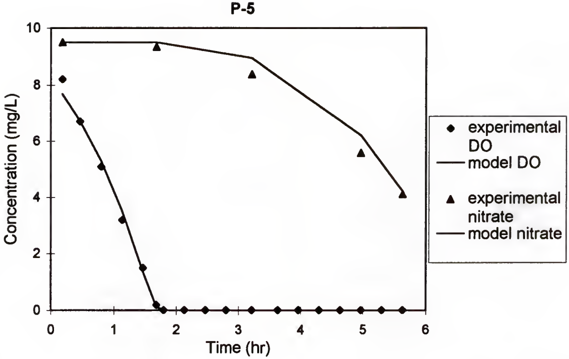

Figure 2.17: Cybernetic model fit to P-5 experimental data: concentration of dissolved oxygen and nitrate.

enzyme concentrations were determined via nonlinear least squares using the performance measure of equation (4). Their values are presented in Table 2.3.

2.5 Discussion

We have shown for the first time that a diauxic lag can be exhibited when activated sludge bacteria switch from oxygen to nitrate as electron acceptors. The cause of the observed diauxies, according to our model, is a low level of denitrifying enzyme (e_{NO}) at the time that dissolved oxygen is depleted (dashed lines in Figure 2.18). The growth rate then approaches zero until the denitrifying enzyme specific level is replenished by biosynthesis. In contrast, when the specific level of denitrifying enzyme is high (e.g., close to its maximum) there is no diauxie (thin lines in Figure 2.18). The dashed lines in Figure 2.18 were obtained by integrating the model with the estimated value $e_{NO}(-7) = 1.4 \times 10^{-4}$ (which results in $e_{NO}(0) = 1.6 \times 10^{-5}$) while the thin lines were obtained by setting $e_{NO}(0) = e_{NO,max} = 2.5 \times 10^{-3}$.

The average duration of the diauxic lags under conditions of the present investigation was over one hour. This is surprising in that it is close to the duration of the anoxic phase in a typical Bio-Denipho process (Zhao *et al.*, 1994), in which case denitrification should be failing. This apparent inconsistency may lie in the differences in the conditions prior to the anoxic phase. From the kinetic rates of Table 2.4 the following expression for the rate of change of e_{NO} in a batch reactor can be obtained:

$$\frac{d\,e_{NO}}{dt} = \frac{\alpha_{NO}\,S_{NO}}{K_{NO}+S_{NO}}\,u_{NO} - \frac{d}{dt}[\ln(X_{BH})]\,e_{NO} - \beta_{NO}\,e_{NO} \qquad (11)$$

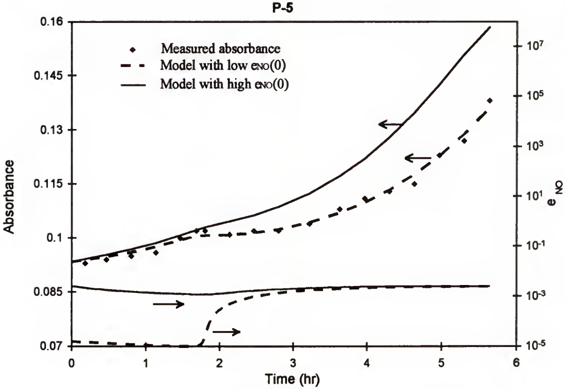

Figure 2.18: Effect of denitrifying enzyme specific level (e_{NO}) on the diauxie.

This shows that specific denitrifying enzyme levels could be depleted due to decay (third term of right-hand side) and "dilution" (second term) as biomass increased exponentially without denitrifying enzyme production (i.e., first term is small). In our work, there was a relatively long aerobic phase that preceded anoxic conditions. (Pre-aeration plus the time it took dissolved oxygen to be exhausted after stopping aeration were three hours or more.) During this period the specific denitrifying enzyme levels could be depleted due to dilution and decay. As we saw previously, with low specific enzyme level a distinct diauxie is predicted. The prior aerobic conditions are different in a full-scale periodic nitrogen removal process, such as Bio-Denipho. First, the heterotrophic bacteria are growing more slowly under carbon limited conditions and hence the rate of enzyme dilution by biomass growth will be lower. Second, the aerobic phases are typically shorter (e.g., 75 min; Zhao et al, 1994). Third, in a full-scale process, the activated sludge experiences anoxic conditions at the bottom of the secondary settling tank, providing the opportunity for regeneration of denitrifying enzymes.

Further research is needed to better define those factors that influence the onset and length of diauxic lags occurring as activated sludge bacteria switch from oxygen to nitrate as oxygen acceptors. Also of importance is the reverse case, i.e., whether or not a diauxic lag occurs when bacteria switch from nitrate to dissolved oxygen as electron acceptor. Based on the present work, caution is urged in the application of conventional models for optimizing periodic processes for nitrogen removal, especially when the tested phase cycling is extrapolated to phase lengths either much shorter or much longer than those tested under experimental conditions.

CHAPTER 3
DIAUXIE OF *PSEUDOMONAS DENITRIFICANS*

3.1 Introduction

According to Monod (1949), who discovered the phenomenon of diauxie or diauxic growth, "This phenomenon is characterized by a double growth cycle consisting of two exponential phases separated by a phase during which the growth rate passes through a minimum, even becoming negative in some cases." Monod (1942) observed diauxic growth when bacteria switch between electron donors, e.g., glucose and sorbitol. Diauxie was subsequently also observed when *Pseudomonas stutzeri* (strain isolated by van Niel and Allen, 1952) switch from nitrate to nitrite as terminal electron acceptor (Kodama *et al.*, 1969).

We recently observed that activated sludge from a full-scale biological process for nitrogen removal (the Bio-Denipho®[†] process at the University of Florida Water Reclamation Facility), grown in the presence of excess carbon substrate, exhibits diauxies with lag phases as long as 2.5 hrs after switching from oxygen to nitrate as terminal electron acceptor (Liu *et al.*, 1996). This may have significant engineering and economic implications since several wastewater treatment processes for nitrogen removal (e.g., sequencing batch reactors, the Bio-Denitro$^{\circledR\dagger}$ process, the Bio-Denipho$^{\circledR\dagger}$ process) periodically switch between oxygen and nitrate as the terminal electron acceptor.

[†] The Bio-Denipho® process is a patented process developed by I Krüger Systems in cooperation with the Department of Environmental Engineering at the Technical University of Denmark (Isaacs *et al.*, 1994).

In the previous experiments with activated sludge it was difficult to ascertain what factors affect the length of the diauxic lag that occurs when the bacteria switch from exponential growth on oxygen to exponential growth on nitrate. To better characterize and understand this phenomenon we conducted experiments with a pure culture of one of the denitrifiers found in activated sludge, Pseudomonas denitrificans. Significant diauxic lags, as long as 7 hours, were observed. Two factors that might affect the length of the lag were investigated. It was determined that the length of the preceding aerated phase has a significant effect, while the presence or absence of nitrate during the aerated phase has a marginal effect.

Diauxic lag caused by switching between carbon sources has been successfully modeled using a cybernetic approach (Ramkrishna, 1982; Ramkrishna *et al.*, 1984; Kompala *et al.*, 1986; Straight and Ramkrishna, 1991; Straight and Ramkrishna, 1994; Ramakrishna *et al.*, 1995) that postulates that bacteria regulate enzyme synthesis and activity so as to maximize their instantaneous specific growth rate. In our previous work (Liu *et al.*, 1996), we showed that incorporating cybernetic expressions for enzyme synthesis and activity in the "industry standard" IAWQ Activated Sludge Model No. 1 enabled us to portray the diauxic lags observed with activated sludge. This model, however, cannot satisfactorily fit the considerably longer lags observed in the present study, neither can it predict the strong dependence of the lag period on the length of the aerated phase. New expressions for enzyme synthesis and activity were therefore developed. The new model successfully portrays the dependence of the diauxic lag on the length of the preceding aerated phase and predicts the observed marginal effect of nitrate presence during the aerated phase.

3.2 Experimental Methods

Freeze-dried culture of *P. denitrificans* (ATCC 13867) was revived in Difco (reorder # 0003-17-8) nutrient broth for three days in a shaking water bath (25°C). The culture was maintained at 4°C on agar plates (10 g/L peptone, 1 g/L yeast extract, 10 g/L NaCl, and 15 g/L agar). Deionized water was used for preparing agar and liquid media. Cultures were grown in a nitrate-free synthetic liquid medium (Table 3.1) modified from Kornaros *et al.* (1996). The pH of the medium was adjusted to 7.0-7.2 with NaOH before autoclaving. Culture medium in 250 ml flasks (125 ml liquid volume) was inoculated from the agar plates, then agitated in a shaker bath for 2 days at approximately 25 °C. The culture was then transferred to a bioreactor and diluted with liquid medium to an absorbance ($\lambda = 550$ nm, 1.25 cm path) of 0.06-0.08 for use in experiments.

Table 3.1. Composition of the synthetic liquid medium

	Chemicals	Deionised water, g/L
Inorganic salts	NaCl	1
	NH_4Cl	1
	$MgSO_4 \cdot 7H_2O$	0.2
	$CaCl_2 \cdot 7H_2O$	0.0264
	Trace metals	a drop*
Phosphates	K_2HPO_4	5
	KH_2PO_4	1.5
Carbon source	L-Glutamic acid	5

*Trace metal solution containing 0.5% (w/v) each of $CuSO_4$, $FeCl_3$, $MnCl_2$, and $Na_2MoO_4 \cdot 2H_2O$

3.2.1 Growth Experiments

Two MultiGen convertible bench-top bioreactors models F-1000 & F-2000 (New Brunswick Scientific) were used for the experiments. Nitrate was added to the bioreactors, with times and quantities varying with the experiment. A drop of antifoam C (Sigma) was also added. The culture was continuously stirred at 30 ± 0.2 °C. The pH ranged from 7.0-7.2 during the experiments. Dissolved oxygen (DO) was monitored using a model DO-40 (New Brunswick Scientific) analyzer with a galvanic electrode. The main feature of the experiment setup was shown in Figure 3.1.

Each experiment consisted of an aeration period of varying length during which dissolved oxygen (7 mg/L or higher) was the terminal electron acceptor. Aeration was then stopped and the reactor was sparged with nitrogen gas to quickly remove the residual dissolved oxygen. Thus followed a period in which nitrate was the terminal electron acceptor. Nitrogen gas was flooded through the head space of the culture bottle during the period in which there was no aeration. Chemical oxygen demand (COD) was measured to ensure that the carbon source (L-glutamic acid) was present in excess at the beginning of the unaerated periods. Other variables monitored included biomass in terms of absorbance, dissolved oxygen, nitrate, and nitrite.

3.2.2 Experimental Protocol

Experiments were carried out in order to investigate the effect of the length of the aeration period and the effect of presence or absence of nitrate during the aeration period on the duration of diauxic lags. Each experiment consisted of two parallel trials with the

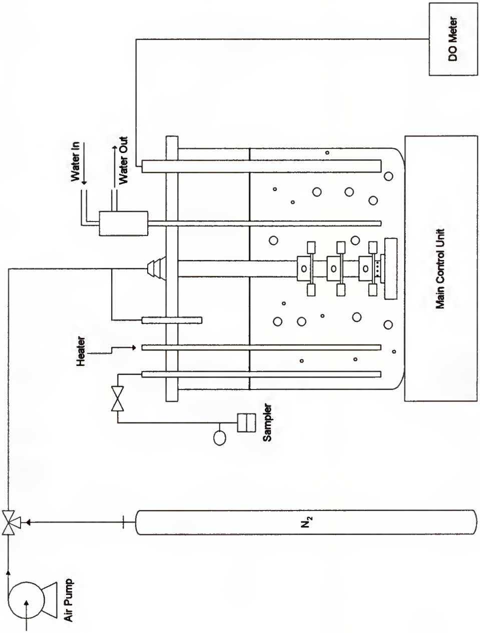
DO Meter
Water In
Water Out
Heater
Main Control Unit
Sampler
N_2
Air Pump

same initial culture conditions (i.e., initial biomass and enzyme concentrations). To ensure that the parallel cultures had the same initial enzyme concentrations, the original culture was well mixed, then divided between the two bioreactors. The first experiment was carried out to determine the effect of the length of the aeration period. Sufficient potassium nitrate was added to given a concentration of 44 mg/L nitrate nitrogen at time zero in both bioreactors. The lengths of aeration in the two parallel bioreactors were 1.1 and 2.55 hours, respectively. The next three experiments were carried out to determine the effect of absence or presence of nitrate during aeration period. In experiment number 2, a nitrate nitrogen concentration of 46 mg/L was added to one bioreactor initially, followed 2.5 hours later with addition at the same concentration to the second bioreactor. In the subsequent two experiments, the dosed nitrate nitrogen concentrations and intervals between addition times were 46-48 mg/L and 2.0-2.5 hours, respectively.

3.2.3 Analytical Methods

Samples were withdrawn from the reactor using a syringe connected to a plastic tube that extended through the cap to the bottom of the reactor. The sample line was initially flushed several times, then 30 mL of culture was withdrawn. A portion (10 mL) of each sample was immediately passed through a membrane filter (Gelman GN-6) having an effective pore size of 0.45 μm and the filtrates were collected and stored at 4°C. Absorbance of the culture was measured with a spectrophotometer (Milton Roy Spectronic 21D) at 550 nm using a 1.25 cm path length.

COD, nitrate and nitrite were measured using test kits (Hach): low range (0 - 150 mg/L) COD test vials, Test 'N Tube NitraVerX nitrate reagent sets (0 - 30 mg/L), and

Test 'N Tube NitriVer3 nitrite test vials (0 - 0.5 mg/L). Six-fold dilution of samples was used to reduce chloride interference on the nitrate measurements. Absorbance was measured at 420 nm for COD, 410 nm for nitrate, and 507 nm for nitrite. Calibration curves were made up for each new set of reagents.

3.3 Experimental Results

The experimental effect of aeration period on the length of diauxic lag is shown by the data points in Figure 3.2 and Figure 3.3. The culture aerated in the presence of nitrate for 1.1 hours experienced a diauxic lag of 3 hours, whereas the culture aerated for a longer time (2.6 hours) experienced a diauxic lag of over 6 hours. The lag periods in both cultures were characterized by low rates of nitrogen consumption (Figure 3.3). The ends of diauxic lag periods were marked by exponential biomass growth and sharply higher nitrate consumption rates.

The experimental effect of the presence of nitrate during the aeration period is shown by the data points in Figure 3.4 and Figure 3.5. The bioreactor containing nitrate from the beginning of the aerated phase (solid triangles) had a marginally shorter diauxic lag (7.5 hours) than the bioreactor to which nitrate was added just prior to stripping out dissolved oxygen (7.8 hours, open circles). Slightly shorter diauxic lag when nitrate was present in the aerated phase was also observed in the two subsequent repetitions (Figure 3.6 and Figure 3.7). Presence of nitrate failed to influence the rate of aerobic growth in either experiment number 2 (Fig. 3.4) or the subsequent two repetitions.

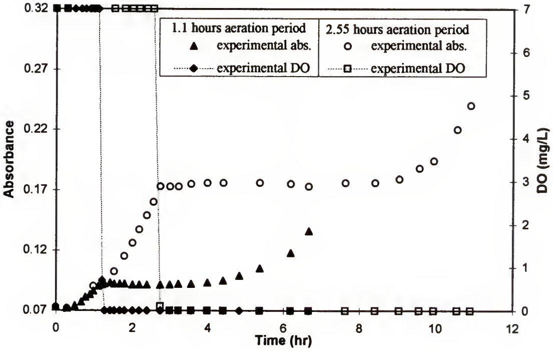

Figure 3.2: Effect of aeration period on the length of the diauxic lag. Data points show experimental results: biomass as indicated by absorbance and dissolved oxygen.

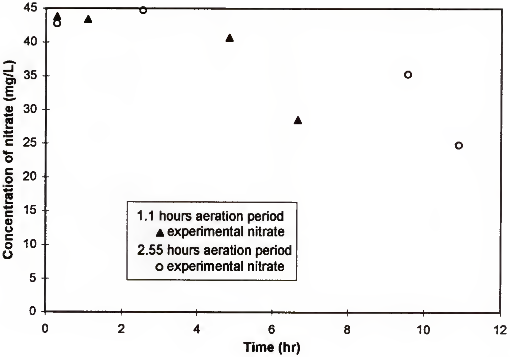

Figure 3.3: Effect of aeration period on the length of the diauxic lag. Data points show experimental results: equivalent nitrate nitrogen concentration.

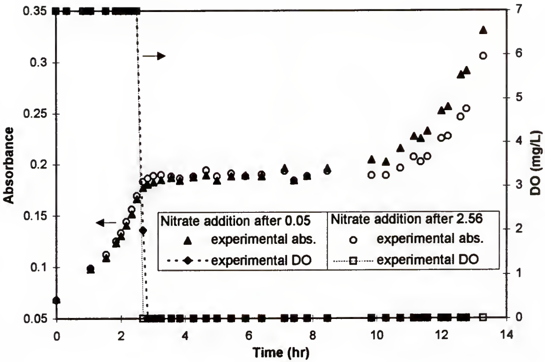

Figure 3.4: Effect of the presence of nitrate during the aeration period. Data points show experimental results: biomass as indicated by absorbance and dissolved oxygen.

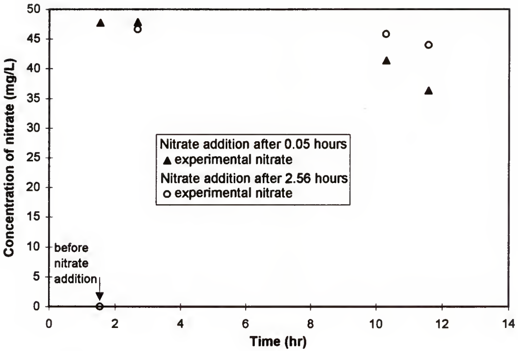

Figure 3.5: Effect of the presence of nitrate during the aeration period. Data points show experimental results: equivalent nitrate nitrogen concentration.

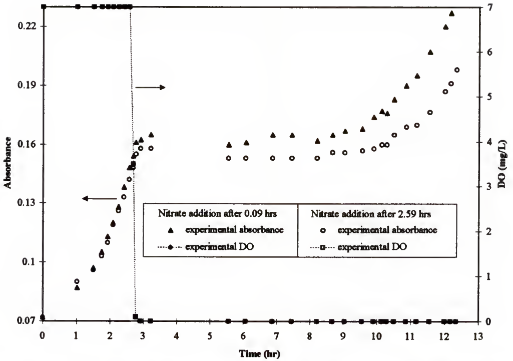

Figure 3.6: Effect of the presence of nitrate during the aeration period. Data points show experimental results: biomass as indicated by absorbance and dissolved oxygen.

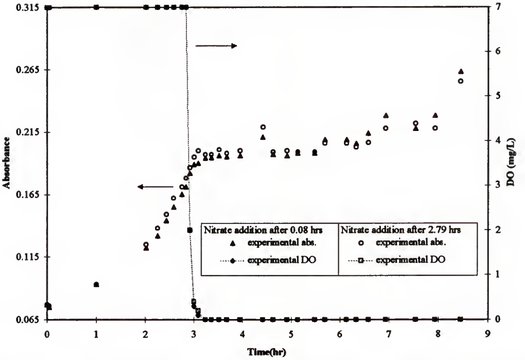

Figure 3.7: Effect of the presence of nitrate during the aeration period. Data points show experimental results: biomass as indicated by absorbance and dissolved oxygen.

3.4 Modeling

We attribute the onset of a diauxic lag to the lack of enzymes needed for electron acceptor utilization (nitrate reductase for the lags shown in Figures 3.2 and Figure 3.4). During the lag period the needed enzyme builds up and when it reaches a sufficient level it becomes activated and exponential growth resumes.

As all experiments were conducted at non-limiting glutamate concentrations, the model presented here does not incorporate the effect of carbon source concentration. The model components are biomass concentration (X_B), dissolved oxygen concentration (S_O), the sum of nitrate plus nitrite nitrogen expressed as equivalent nitrate nitrogen concentration (S_{NO}), and the concentrations of two enzymes, E_O and E_{NO}, which catalyse biomass synthesis on oxygen and nitrate, respectively. Equivalent nitrate nitrogen concentration (S_{NO}) is calculated from:

$$S_{NO} = [NO_3 - N] + \frac{(2.857 - 1.143)}{2.857}[NO_2 - N] \tag{1}$$

The model considers the following processes: aerobic (utilizing oxygen) synthesis of biomass, anoxic (utilizing nitrate) synthesis of biomass, synthesis of the two enzymes, decay of biomass, and decay of the two enzymes.

The rate of biomass synthesis under anoxic conditions is given by:

$$\rho_{NO} = \hat{\mu}_{H,NO} \frac{e_{NO}\, v_{NO}}{e_{NO,max}} \left(\frac{S_{NO}}{K_{NO} + S_{NO}} \right) X_B \tag{2}$$

The effect of nitrate on the rate of biomass synthesis is given by a Monod-type switching function, with $\hat{\mu}_{H,NO}$ representing the maximum specific growth rate, K_{NO} the nitrate half-saturation coefficient for biomass synthesis, and X_B the biomass concentration. The effect of nitrate reductase on anoxic biomass synthesis is portrayed as the product of relative enzyme level and enzyme activity. The variable e_{NO} represents the specific enzyme level $e_{NO} = E_{NO}/X_B$, and $e_{NO,max}$ its maximum attainable value. The variable v_{NO} ranges from 0 to 1 and represents enzyme activity. Thus the specific growth rate attains its maximum value for given nitrate concentration only when the enzyme specific level is at its maximum and fully activated. An analogous expression is used for aerobic biomass synthesis, with oxygen replacing nitrate.

The nitrate reductase synthesis rate is given by:

$$(\alpha_{NO,1} + \alpha_{NO,2} \frac{e_{NO}}{e_{NO,max}}) u_{NO} \left(\frac{S_{NO}}{K_{NO} + S_{NO}} \right) X_B \qquad (3)$$

This has the same Monod dependence on nitrate as the biomass synthesis rate. The variable u_{NO} has values between 0 and 1 and controls enzyme induction. As in the cybernetic models (Kompala et al., 1986) it is assumed (for inducible enzymes) that resources for enzyme synthesis are allocated in proportion to the biomass specific growth rate for fully active enzymes, which yields the expression:

$$u_{NO} = \frac{\rho_{NO} / v_{NO}}{\rho_O / v_O + \rho_{NO} / v_{NO}} \qquad (4)$$

In contrast to the cybernetic models, however, the leading coefficient of equation (3) is not constant but an increasing function of enzyme specific level. At low enzyme specific levels, low amount of energy will be available for biosynthesis. Increasing enzyme level would therefore increase available energy and thus the potential enzyme synthesis rate. Furthermore, at higher the enzyme specific levels, more metabolic machinery will be available for utilizing this energy, therefore increasing the efficiency of enzyme synthesis.

The expression for enzyme activity, v_{NO}, also differs from the one used in the cybernetic models. It provides for a sharper transition from inactive to active enzyme by utilizing a logistic function of the ratio $e_{NO}/e_{NO,max}$:

$$v_{NO} = \frac{1}{1+e^{4s\left(r_{c,NO} - \frac{e_{NO}}{e_{NO,max}}\right)}} \tag{5}$$

For large values of the parameter s, v_{NO} is close to zero (inactive enzyme) for ratio $e_{NO}/e_{NO,max} = 0$ and close to one (full activation) for $e_{NO}/e_{NO,max} = 1$. As Figure 3.8 shows, the parameter $r_{c,NO}$ (critical ratio) sets the value of the ratio for which enzyme activity reaches 50%. The parameter s (sharpness parameter) is the slope of the curve at $e_{NO}/e_{NO,max} = r_{c,NO}$.

The model also includes an enzyme decay rate, which is proportional to the enzyme concentration: $\rho_{decay} = \beta_{NO} E_{NO}$.

The maximum enzyme specific level is not an independent parameter. It is the specific level attained when nitrate is nonlimiting and oxygen is absent (in which case $u_{NO} = 1$), and it can be readily calculated from the material balance on E_{NO} as:

$$e_{NO,max} = \frac{\alpha_{NO,1} + \alpha_{NO,2}}{\hat{\mu}_{H,NO} + \beta_{NO} - b_H} \tag{6}$$

An issue is whether or not nitrate reductase is synthesized during an aerobic phase if nitrate is present. Our model predicts that it is, although since enzyme synthesis does not keep up with biomass synthesis, the nitrate reductase specific level drops when oxygen is present. The model can be changed to portray negligible synthesis of the reductase by multiplying the anoxic biomass synthesis rate (eq. 2) and the related enzyme synthesis rate

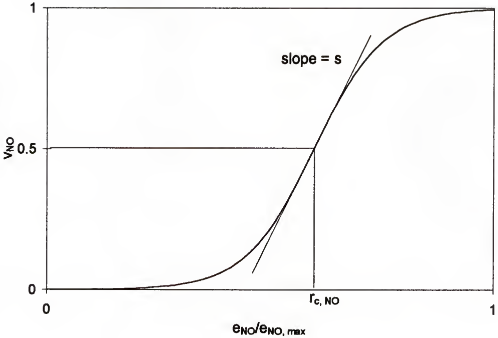

Figure 3.8: Effect of enzyme concentration on enzyme activity, v_{NO}.

(eq. 3) by $K_{O,H}/(S_O+K_{O,H})$, an oxygen inhibition term used in an industry-standard model for activated sludge (Henze *et al.*, 1987). The model would then predict no difference in the length of the diauxic lag and biomass growth between the cases of nitrate present and nitrate absent during aerobic growth, whereas small differences were observed experimentally. Furthermore, this would contradict the work of Simpkin and Boyle (1988) who determined that repression by oxygen of the synthesis of the denitrifying enzymes is not complete in activated sludge. For these reasons, this oxygen inhibition term is not incorporated in our model.

Regarding aerobic growth, if the oxygenase is an inducible enzyme, expressions analogous to those for the nitrate reductase are applicable. If, on the other hand, it is a constitutive enzyme, then the induction variable u_O is identically equal to 1. Setting the initial enzyme specific level equal to $e_{O,max}$ (given by an analogue of equation 6) then results in e_O being always equal to its maximum value. Furthermore, the analogue of equation (5) would then yield $v_O \cong 1$, i.e. that the enzyme is fully activated. Then the aerobic biomass growth rate reduces to a conventional Monod expression, without any effects from the enzyme. If the oxygenase were inducible, there would be a diauxic lag when *P. denitrificans* switches from nitrate to oxygen as terminal electron acceptor. A preliminary experiment was inconclusive, showing perhaps a very short lag (< 10 min).

The complete kinetic model, assuming that both enzymes are inducible, is summarized in Table 3.2. Note that different yield coefficients are used for aerobic and anoxic growth. This is supported by the work of Koike and Hatori (1975). As mentioned previously, the model assumes that the carbon source is present in excess and therefore

Table 3.2. Process kinetics and stoichiometry of the new model

Component→	i	1	2	3	4	5	
j	Process ↓	S_O	S_{NO}	X_B	E_O	E_{NO}	Process rate, ρ_j, $ML^{-3}T^{-1}$
1	Aerobic growth	$-\frac{1-Y_{H,O}}{Y_{H,O}}$		1			$\hat{\mu}_{H,O}\frac{e_O \mathrm{v}_O}{e_{O,max}}\left(\frac{S_O}{K_{O,H}+S_O}\right)X_B$
2	Anoxic growth		$-\frac{1-Y_{H,NO}}{2.86Y_{H,NO}}$	1			$\hat{\mu}_{H,NO}\frac{e_{NO} \mathrm{v}_{NO}}{e_{NO,max}}\left(\frac{S_{NO}}{K_{NO}+S_{NO}}\right)X_B$
3	Decay			-1			$b_H X_B$
4	Synthesis rate of enzyme associated with aerobic growth				1		$\left[\alpha_{O,1}+\alpha_{O,2}\frac{e_O}{e_{O,max}}\right]\left(\frac{S_O}{K_{O,H}+S_O}\right)X_B \mathrm{u}_O$
5	Synthesis rate of enzyme associated with anoxic growth					1	$\left[\alpha_{NO,1}+\alpha_{NO,2}\frac{e_{NO}}{e_{NO,max}}\right]\left(\frac{S_{NO}}{K_{NO}+S_{NO}}\right)X_B \mathrm{u}_{NO}$
6	Enzyme decay rate				-1		$\beta_O E_O$
7	Enzyme decay rate					-1	$\beta_{NO} E_{NO}$
Observed conversion rate, $ML^{-3}T^{-1}$		$r_i=\sum_j \gamma_{ij}\rho_j$					

Model Relationships

$$\mathrm{v}_i = \frac{1}{1+e^{4s\left(r_{c,i}-\frac{e_i}{e_{i,max}}\right)}}$$

$$\mathrm{u}_i = \frac{\rho_i/\mathrm{v}_i}{\sum_{i=1}^{2}(\rho_i/\mathrm{v}_i)}$$

$$e_i = \frac{E_i}{X_B}$$

$$e_{i,max} = \frac{\alpha_{i,1}+\alpha_{i,2}}{\hat{\mu}_{max,i}+\beta_i-b_H}$$

where

$i = O$ or NO

$\rho_O = \rho_1$

$\rho_{NO} = \rho_2$

neither of the process rate expressions for growth contains a substrate concentration term, nor is substrate shown as a component.

As Figure 3.9 and Figure 3.10 shows, the model of Table 3.2 fits very well the experimental results obtained by varying the length of the aeration period. The model correctly predicts that the longer the aeration period is, the longer will the diauxic lag be, and it also fits well both the biomass and nitrate concentration profiles. Dissolved oxygen was not predicted by the model because DO was stripped out after stopping aeration. The values for the model parameters (maximum specific growth rate with oxygen $\hat{\mu}_{H,O}$, maximum specific growth with nitrate $\hat{\mu}_{H,NO}$, yield coefficients $Y_{H,O}$ and $Y_{H,NO}$, half saturation coefficients $K_{O,H}$ and K_{NO}, decay rate b_H, enzyme decay coefficients β_O and β_{NO}, enzyme synthesis coefficients $\alpha_{NO,1}$, $\alpha_{NO,2}$, $\alpha_{O,1}$, and $\alpha_{O,2}$, sharpness parameter s, and critical ratios $r_{c,O}$ and $r_{c,NO}$) as well as the initial concentration of biomass and initial enzyme concentrations were determined by nonlinear weighted least squares fitting using the following performance measure:

$$J = \frac{1}{\sigma_{S_{NO}}^2} \sum_j (S_{NOmeas,j} - S_{NOpred,j})^2 + \frac{1}{\sigma_A^2} \sum_\ell (A_{meas,\ell} - A_{pred,\ell})^2 \tag{7}$$

where $\sigma_{S_{NO}} = 0.5\,mg/L \; and \; \sigma_A = 0.001$ are the standard deviations of the nitrate-nitrogen and absorbance (A) measurements, respectively. The parameter and initial values are shown in Tables 3.3 and 3.4, respectively.

Table 3.3 also shows an estimate of the standard deviation of the parameter values. There are 59 experimental points in Figure 3.9 and 3.10 and these were used to fit 16

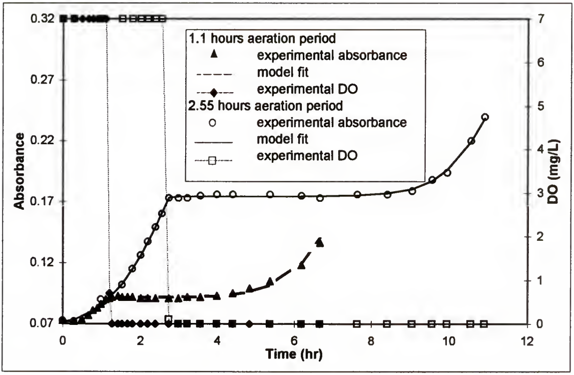

Figure 3.9: Effect of aeration period on the length of the diauxic lag. Data points show experimental results, dash and solid lines show model fits: biomass as indicated by absorbance and dissolved oxygen.

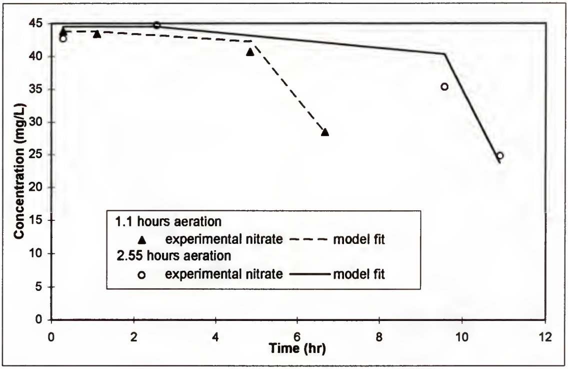

Figure 3.10: Effect of aeration period on the length of the diauxic lag. Data points show experimental results, dash and solid lines show model fits: equivalent nitrate nitrogen concentration.

Table 3.3. Model parameter values

Parameter	Symbol	Units	Value	Estimated Std. Dev.
Maximum Specific Rates				
Growth in DO	$\hat{\mu}_{H,O}$	hr^{-1}	0.342	$5.53e^{-4}$
Growth in nitrate	$\hat{\mu}_{H,NO}$	hr^{-1}	0.322	$7.29e^{-4}$
Yields				
in DO phase	$Y_{H,O}$	g cell COD / g substrate COD	0.703	$9.44e^{-3}$
in nitrate phase	$Y_{H,NO}$	g cell COD / g substrate COD	0.570	0.012
Half Saturation Coefficients				
Oxygen coeff.	$K_{O,H}$	$g\ O_2\ m^{-3}$	0.373	0.020
Nitrate coeff.	K_{NO}	$g\ NO_3\text{-}N\ m^{-3}$	0.326	0.049
Biomass Specific Decay Rate	b_H	hr^{-1}	0.0	$2.17e^{-4}$
Enzyme Specific Synthesis Rates				
DO	$\alpha_{O,1}$	hr^{-1}	$8.90e^{-4}$	$3.37e^{-6}$
	$\alpha_{O,2}$	hr^{-1}	$1.69e^{-5}$	$2.73e^{-6}$
Nitrate	$\alpha_{NO,1}$	hr^{-1}	$2.16e^{-7}$	$9.99e^{-9}$
	$\alpha_{NO,2}$	hr^{-1}	$3.65e^{-5}$	$2.13e^{-7}$
Enzyme Specific Decay Rates				
DO	β_O	hr^{-1}	0.0	$1.14e^{-3}$
Nitrate	β_{NO}	hr^{-1}	0.537	0.011
Critical Ratio				
DO	$r_{c,O}$		0.666	$1.87e^{-3}$
Nitrate	$r_{c,NO}$		0.604	$3.94e^{-3}$
Sharpness Parameter	s		2.7	0.044

Table 3.4. Model initial conditions

Parameter	Symbol	Units	Values in the model 1st Exp.	 2nd Exp.
Initial Biomass Concentration	X_B	g COD m^{-3}	238	224
Initial Specific Enzyme Levels				
DO	e_O	g enzyme / g biomass	0.00135	0.00156
Nitrate	e_{NO}	g enzyme / g biomass	0.000011	0.0000077

parameter values and 3 initial conditions. If the measurements were independently distributed, then the standard deviation of parameter θ_i is approximately (Seber and Wild, 1989)

$$s_{\theta_i} = \sqrt{Q_{ii}} \tag{8}$$

where Q_{ii} is the i^{th} diagonal element of

$$Q = \frac{J(\underline{\theta}^*)}{59-19}[F^T(\underline{\theta}^*)F(\underline{\theta}^*)]^{-1} \tag{9}$$

Here $\underline{\theta}^*$ is the vector of optimal parameter values and F is the Jacobian with ij^{th} element.

$$f_{ij} = \left.\frac{\partial f(t_i, \underline{\theta})}{\partial \theta_j}\right|_{\underline{\theta}=\underline{\theta}^*} \tag{10}$$

The function $f(t_i, \underline{\theta})$ is the implicit relationship between a normalized measurement (absorbance/σ_A or nitrate-nitrogen/$\sigma_{S_{NO}}$) and time, where t_i is the time for the i^{th} measurement. The terms f_{ij} were calculated by numerical differentiation. As the assumption of independently distributed measurement is not satisfied, the s_{θ_i} calculated can only be viewed as rough indicators of the uncertainty in the parameter values.

In contrast to the new model, the previous cybernetic model cannot fit satisfactorily the experimental results as shown in Figure 3.11. The cybernetic model is unable to fit a long diauxic lag, and neither can it portray its strong dependence on the length of the aeration period.

The parameter values of Table 3.3 were subsequently used to predict the performance of the culture for the experiments investigating the effect of the presence or

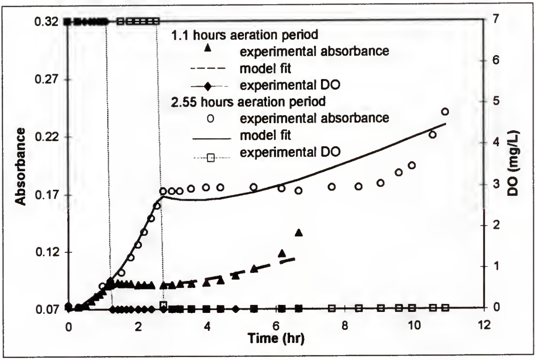

Figure 3.11: Effect of aeration period on the length of the diauxic lag. Data points show experimental results, dash and solid lines show cybernetic model fits: biomass as indicated by absorbance and dissolved oxygen.

absence of nitrate during the aeration period. The initial values of biomass concentration and enzyme levels were determined by nonlinear least squares fitting as described above, and are also shown in Table 3.4. As shown in Figure 3.12 and Figure 3.13, the model predicts successfully both biomass absorbance and nitrate uptake. It also predicts that a slightly shorter diauxic lag results when nitrate is present during the aerated phase, as observed in Figure 3.12 as well as in the two repetitions (not shown). Finally, the model predicts a slightly lower aerobic growth rate when nitrate is present, something in agreement with previous work of Simpkin and Boyle (1988) and Kornaros and Lyberatos, (1997).

3.5 Conclusions

We have shown that diauxie occurs when *Pseudomonas denitrificans* switch between oxygen and nitrate as terminal electron acceptor. Experiments with pure culture also showed that the length of the aeration period significantly affects the length of the diauxic lag, whereas the presence or absence of nitrate during the aerating phase has a marginal effect. A new model accounting for enzyme synthesis and activity was developed. This fits very well the experimental results with respect to both biomass growth and nitrate uptake, and correctly predicts the length of the observed diauxic lags.

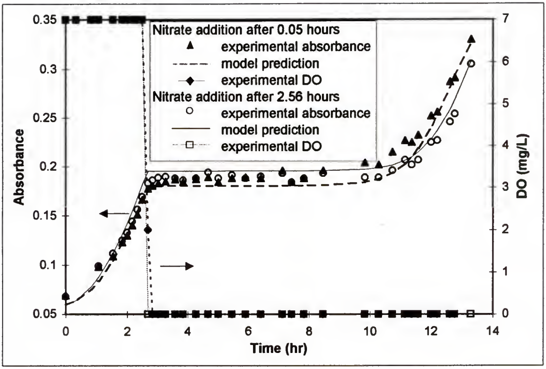

Figure 3.12: Effect of the presence of nitrate during the aeration period. Data points show experimental results, dash and solid lines show model predictions: biomass as indicated by absorbance and dissolved oxygen.

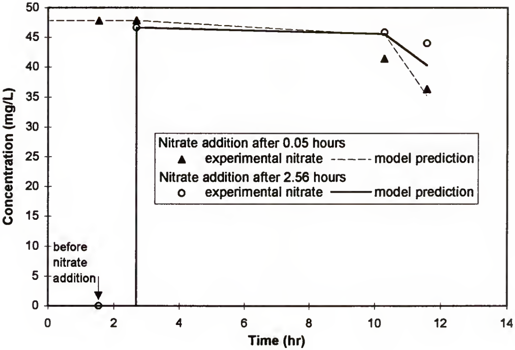

Figure 3.13: Effect of the presence of nitrate during the aeration period. Data points show experimental results, dash and solid lines show model predictions: equivalent nitrate nitrogen concentration.

CONCLUSIONS & FUTURE WORKS

Up to now, the potential for growth lag caused by switching between electron acceptors in periodically operated wastewater treatment plants has not been recognized, even though these facilities are becoming increasingly popular because of their flexibility and economy. Our work has shown that significant lags occur both in activated sludge and in pure cultures of denitrifying bacteria. Because standard models do not account for diauxic lags, their results in optimizing operation of periodically operated plants could be misleading. Our modeling work, for the first time, introduces the ability to depict the effect of operating conditions on diauxic lags, and represents an important step towards understanding the importance of this phenomenon in nitrogen-removing wastewater treatment plants.

There remain considerable issues to be investigated. All experiments in the present work were considered with nonlimiting carbon source. The effect of the substrate concentration on the length of diauxic lag should be investigated. Also, the age of the pure culture may have a significant effect on the onset of diauxie. Experiments should be designed and conducted to better understand this effect.

Finally, although there is some previous work showing that diauxies could also happen when bacteria switch from nitrate to nitrite as terminal electron acceptor, preliminary experiments with *Pseudomonas denitrificans* by our group failed to detect it.

This diauxie (from nitrate to nitrite) should be studied further, and the applicability of our model investigated.

LIST OF REFERENCES

Baloo S. and Ramkrishna D. (1991) Metabolic Regulation in Bacterial Continuous Cultures: II. *Biotechnol. Bioeng.* **38**, 1353-1363.

Bundgaard E. and Pedersen (1991) Techniques for and Experience with Biological Nutrient Removal – Danish Long-Term Operating and Optimization Experience. *Wat. Sci. Tech.* **24**, 10, 211-216.

Bundgaard E., Andersen K. L., and Petersen G. (1989) Bio-Denitro and Bio-Denipho Systems – Experimences and Advanced Model Development: The Danish Systems for Biological N and P Removal. *Wat. Sci. Tech.* **21**, 1727-1730.

Dijkhuizen L., van der Werf B., and Harder W. (1980) Metabolic Regulation in Pseudomonas Oxaliticus OX1. Diauxic Growth on Mixtures of Oxalate and Formate or Acetate. *Arch. Microbiol.* **124**, 261-268.

Harder W. and Dijkhuizen L. (1982) Strategies of Mixed Substrate Utilization in Microorganisms. *Phil. Trans. Royal Soc. Lond.* **B 297**, 459-480.

Henze M., Grady C. P. L., Gujer W., Marais G. v. R., and Matsuo T. (1987) Activated Sludge Model No. 1. *IAWPRC Scient. Tech. Rep. No. 1.* IAWPRC London, U.K.

Henze M., Gujer W., Mino T., Matsuo T., Wentzel M. C., and Marais G. v. R. (1995) Activated Sludge Model No. 2. *IAWQ Scient. Tech. Rep. No. 3.* IAWQ London.

Isaacs S. H., Henze M., Søeberg H., and Kümmel M. (1994) External Carbon Source Addition as a Means to Control an Activated Sludge Nutrient Removal Process. *Wat. Res.* **28**, 511-520.

Kodama T., Shimada K., and Mori T. (1969) Studies on Anaerobic Biphasic Growth of Denitrifying Bacterium, *Pseudomonas stutzeri. Plant & Cell Physiol.* **10**, 855-865.

Koike I. and Hattori A. (1975) Growth Yield of a Denitrifying Bacterium, Pseudomonas denitrificans, under Aerobic and Denitrifying Conditions. *J. Gen. Microbiol.* **88**, 1-10.

Kompala D. S., Ramkrishna D., Jansen N. B., and Tsao G. T. (1986) Investigation of Bacterial Growth on Mixed Substrates: Experimental Evaluation of Cybernetic Models. *Biotechnol. Bioeng.* **28**, 1044-1055.

Kornaros M. and Lyberatos G. (1997) Kinetics of Aerobic Growth of a Denitrifying Bacterium, *Pseudomonas Denitrificans*, in the Presence of Nitrates and/or Nitrites. *Wat. Res.* **31**, 3, 479-488.

Kornaros M., Zafiri G., and Lyberatos G. (1996) Kinetics of Denitrification by *Pseudomonas Denitrificans* under Growth Conditions Limits by Carbon and/or Nitrate or Nitrite. *Wat. Env. Res.* **68**, 5, 934-945.

Liu, P., Zhan, G., Svoronos, S. A., and Koopman, B. (1996) Cybernetic Approach to Modeling Denitrification in Activated Sludge. Presented at the *1996 AIChE National Meeting*, Chicago.

Meiberg B. M., Bruinenberg P. M., and Harder W. (1980) Effect of Dissolved Oxygen Tension on the Metabolism of Methylated Amines in Hyphomicrobium X in the Absence and Presence of Nitrate: Evidence for the 'Aerobic' Denitrification. *J. of Gen. Microbiol.* **120**, 453-463.

Monod J. (1942) Recherches sur la Croissance des Cultures Bacteriénnes. *Actualités Scientifique et Industrielles* **911**, 1-215.

Monod J. (1949) The Growth of Bacterial Cultures. *Annual Review of Microbiol.*, Clifton C. E., Raffel S., Barker H. A., Eds. **3**, 371-394.

Nikolajsen K., Nielsen J., and Villadsen J. (1991) Structured Modeling of a Microbial System: III. Growth on Mixed Substrates. *Biotechnol. Bioeng.* **38**, 24-29.

Potter T. G., Koopman B., Svoronos S. A. (1996) Optimization of a Periodic Biological Process for Nitrogen Removal from Wastewater. *Wat. Res.* **30**, 142-152.

Ramakrishna R., Ramkrishna D., and Konopka A. E. (1995) Cybernetic Modeling of Growth in Mixed, Substitutable Substrate Environments. Preferential and Simultaneous Utilization. Presented at the *1995 AIChE National Meeting*, Miami Beach.

Ramkrishna D. (1982) A Cybernetic Perspective of Microbial Growth. in Foundations of Biochemical Eng. in *Kinetics and Thermodynamics in Biological Systems.*, Papoutsakis E. I., Stephanopoulos G. N., and Blanch H. W., Eds. American Chemical Society, Washington, D.C., 161-178.

Ramkrishna D., Kompala D. S., and Tsao G. T. (1984) Cybernetic Modeling of Microbial Populations. in *Frontiers in Chemical Reaction Eng.*, Doraiswamy L. K., and Mashelkar R. A., Eds. Wiley Eastern Limited, New Delhi 1.

Ramkrishna D., Kompala D. S., and Tsao G. T. (1987) Are Microbes Optimal Strategists? *Biotechnol. Progress* **3**, 121-126.

Seber G. A. F. and Wild C. J. (1989) Nonlinear Regression. John Wiley & Sons, New York.

Simpkin T. J., and Boyle W. C. (1988) The Lack of Repression by Oxygen of the Denitrifying Enzymes in Activated Sludge. Wat. Res. **22**, 2, 201-206.

Straight J. V. and Ramkrishna D. (1991) Complex Growth Dynamics in Batch Cultures: Experiments and Cybernetic Models. *Biotechnol. Bioeng.* **37**, 895-909.

Straight J. V. and Ramkrishna D. (1994) Cybernetic Modeling and Regulation of Metabolic Pathways. Growth on Complementary Nutrients. *Biotechnol. Prog.* **10**, 574-587.

Van Dedem G. and Moo-Young M. (1975) A Model for Diauxic Growth. *Biotechnol. Bioeng.* **17**, 1301-1312.

van Niel C. B. and Allen M. B. (1952) A Note on *Pseudomonas stutzeri*. *J. Bacteriol.* **64**, 413-422.

Williamson K. J. and McCarty P. L. (1975) Rapid Measurement of Monod Half-Velocity Coefficients for Bacterial Kinetics. *Biotechnol. Bioeng.* **17**, 915-924.

Zhao H., Isaacs S. H., Søeberg H., and Kümmel M. (1994) A Novel Control Strategy for Improved Nitrogen Removal in an Alternating Activated Sludge Process-Part I. Process Analysis. *Wat. Res.* **28**, 521-534.

BIOGRAPHICAL SKETCH

Pi-Hsin Liu was born on March 1, 1971, in Kaohsiung, Taiwan. She received her Bachelor degree in chemical engineering from the National Tsing-Hua University in Hsin-Chu, Taiwan. In 1993, she was accepted to the University of Florida Department of Chemical Engineering in Gainesville, Florida, to pursue a degree of Doctor of Philosophy.

I certify that I have read this study and that in my opinion it conforms to acceptable standards of scholarly presentation and is fully adequate, in scope and quality, as a dissertation for the degree of Doctor of Philosophy.

Spyros A. Svoronos

Spyros A. Svoronos, Chairman
Professor of Chemical Engineering

I certify that I have read this study and that in my opinion it conforms to acceptable standards of scholarly presentation and is fully adequate, in scope and quality, as a dissertation for the degree of Doctor of Philosophy.

Ben Koopman, Cochairman
Professor of Environmental
Engineering Sciences

I certify that I have read this study and that in my opinion it conforms to acceptable standards of scholarly presentation and is fully adequate, in scope and quality, as a dissertation for the degree of Doctor of Philosophy.

Paul A. Chadik
Assistant Professor of Environmental
Engineering Sciences

I certify that I have read this study and that in my opinion it conforms to acceptable standards of scholarly presentation and is fully adequate, in scope and quality, as a dissertation for the degree of Doctor of Philosophy.

Richard Dickinson
Assistant Professor of Chemical
Engineering

I certify that I have read this study and that in my opinion it conforms to acceptable standards of scholarly presentation and is fully adequate, in scope and quality, as a dissertation for the degree of Doctor of Philosophy.

Gar B Hoflund

Gar Hoflund
Professor of Chemical Engineering

I certify that I have read this study and that in my opinion it conforms to acceptable standards of scholarly presentation and is fully adequate, in scope and quality, as a dissertation for the degree of Doctor of Philosophy.

Dale Kirmse
Associate Professor of Chemical
Engineering

This dissertation was submitted to the Graduate Faculty of the College of Engineering and to the Graduate School and was accepted as partial fulfillment of the requirements for the degree of Doctor of Philosophy.

May 1998

Winfred M. Phillips
Dean, College of Engineering

Karen A. Holbrook
Dean, Graduate School